논문 2012-49-9-18

기준신호원을 이용한 배열센서의 위치, 이득, 위상 보정기법

(Location and Gain/Phase Calibration Techniques for Array Sensors with known Sources)

유 성 기*, 이 태 범*, 신 기 영**

(Seong Ki Yoo, Tae Beom Lee, and Ki Young Shin)

요 약

기하학적 오차와 전기적 오차는 배열센서 시스템의 성능을 심각하게 저하할 수 있다. 이러한 문제를 완화시키기 위해 다양한 보정 기술이 개발되었다. 본 논문에서는 배열센서의 위치오차, 이득오차, 위상오차를 보상하는 두 가지 기술을 비교하였다. 그 중 하나의 방법은 1차 테일러급수 전개를 통해 배열센서의 명목상 값으로부터 실제 조향 벡터를 예측한 후 MUSIC 알고리즘의 null 특성을 이용하여 형성되는 몇 가지 식을 이용하여 센서의 실제 위치, 이득, 위상을 추정한다. 또 다른 하나의 방법은 기준신호원의 공분산 행렬을 이용하여 이러한 오차들을 예측한다. 시뮬레이션을 통해 두 가지 보정기술 모두 성공적으로 오차를 보정하였고, 10dB~50dB SNR 범위에서 Fistas and Manikas의 알고리즘이 Ng and Lie의 알고리즘 보다 노이즈에 더 강건하다는 것을 증명하였다.

Abstract

The geometrical and electrical errors of array sensors can severely degrade the performance of array sensor system. Various calibration techniques are developed to alleviate this problem. In this paper, two different calibration methods with respect to location, gain and phase of array sensors are presented. One method applies the first-order Taylor series expansion to approximate the true steering vector from the nominal values of array sensors. Then a set of equations is formed by using the null characteristics of the MUSIC spectrum to estimate errors of location, gain and phase of array sensors. Another method estimates these errors based on the data covariance matrix of pilot sources. From the simulations, it is demonstrated that two calibration algorithms calibrated an array system successfully. In addition to that, Fistas and Manikas's algorithm is more robust against noise than Ng and Lie's one when SNR is from 10dB to 50dB.

Keywords : Array Calibration. Geometrical and electrical errors, Maximum likelihood estimation, Known sources, Root mean square errors

I. Introduction

Array signal processing techniques are based on the a priori knowledge of the geometrical and electrical sensor characteristics with assumption that they are accurate. In practical systems, however, this assumption is no longer satisfied. This is because geometrical (sensor location) and electrical (gain and phase) errors/uncertainties are inherent in the manufacturing process of sensor array. In other words, array signal processing techniques in practice have been limited due to the fact that calibration errors relate to gemetrical and electrical characteristics of array. These errors cause the severe degradation of their performance[1~2]. Hence,

* 정회원, ** 정회원-교신저자, 한국전기연구원
(Korea Electrotechnology Research Institute)
※ 이 논문은 지식경제부의 산업원천기술개발사업 지원으로 수행되었음. (과제번호 : 10028436)
접수일자: 2012년3월7일, 수정완료일: 2012년5월24일

various approaches have been studied and presented, so as to identify these errors and rectify the knowledge of the actual sensor characteristics, this process is called array calibration. These calibration techniques are either applicable in only array sensor location errors[3~9] or only array sensor gain/phase errors[10~13]. In practice, however, it is more likely to have both electrical and geometrical errors in array sensors. Therefore, global array calibration methods[14~16] which calibrate an array system with respect to errors in location, phase and gain by using emitting sources with known direction-of-arrival (DOA's) are developed. The main idea of the array calibration technique designed by Ng and Lie[14] is to apply the first-order Taylor series expansion to approximate the true array steering vector from the nominal values of array sensors. Then a set of linear equations is formed, using the null property of the MUSIC (Multiple Signal Classification) spectrum, from which the difference between the actual steering vector and the nominal steering vector. On the other hand, Fistas and Manikas[15] present a new array calibration method based on the data covariance matrix of a pilot source. The purpose of this paper is to demonstrate which algorithm is more robust in noise environment.

In Section Ⅱ, the mathematical signal modelling and the array calibration technique of each methods are presented. Then, in Section Ⅲ, the performance of two different methods are demonstrated and compared by the computer-based simulation results. In this section, two calibration techniques are compared with respect to root-mean-square-errors (RMSE) of location, gain and phase with different value of signal-to-noise ratio (SNR). Finally, in Section Ⅳ, the conclusion of this paper is made.

Ⅱ. Mathematical Model and Array Calibration Method

2-1. Fistas and Manikas' s method

Consider an array of N sensors that operate in the presence of one pilot source of unity power at azimuth angle of θ and elevation angle of ϕ as shown in Fig. 1. In the ideal case, the array data covariance matrix R_{xx} can be expressed as follows:

$$\widehat{R_{xx}} = \underline{S} \cdot \underline{S}^H + R_{nn} \tag{1}$$

where $\underline{S}$ is the source position vector (SPV) or array manifold vector and R_{nn} is the noise covariance matrix. R_{nn} can be equal to $\sigma^2 I_N$, with assumption that the noise is isotropic and un-correlated from sensor to sensor, where σ^2 is the power of noise and I_N is the identity matrix with size of $N \times N$.

In the practical application, however, the data covariance matrix associated with geometrical and electrical errors can be expressed as:

$$\begin{aligned}\widehat{R_{xx}} &= (\underline{S} + \tilde{\underline{S}}) \cdot (\underline{S} + \tilde{\underline{S}})^H + \sigma^2 I_N \\ &= (I + \widetilde{\Delta}) \cdot \underline{S} \cdot \underline{S}^H \cdot (I + \widetilde{\Delta}) + \sigma^2 I_N \end{aligned} \tag{2}$$

In this calibration method, it is needed to define a new matrix O in terms of the nominal values for the phase of the array($\underline{\psi}$) and SPV corresponding to the pilot source($\underline{a}$):

$$O = \mathrm{diag}(\underline{\psi} \odot \underline{a}) \tag{3}$$

Then the following matrix can be established by pre- and post-processing the data covariance matrix

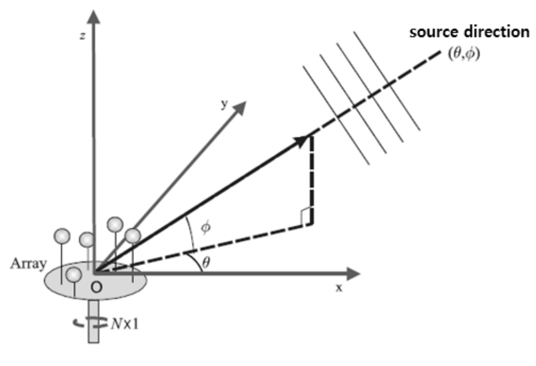

그림 1. 신호원과 배열센서의 상대적인 위치
Fig. 1. Relative geometry between an emitting source and an array of sensors.

$\widehat{R_{xx}}$ by the defined matrix O above:

$$O^H \cdot \widehat{R_{xx}} \cdot O = diag(U) \cdot diag(U)^H + \sigma^2 I_N \tag{4}$$

where $U = (I + \widetilde{\triangle}) \cdot diag(\underline{\gamma}) = \boldsymbol{\Gamma} \cdot \widetilde{\boldsymbol{\Psi}} \cdot \widetilde{A}$

and $\boldsymbol{\Gamma} = diag(\underline{\gamma} + \underline{\tilde{\gamma}})$,
$\widetilde{\boldsymbol{\Psi}} = diag(\underline{\tilde{\psi}})$, and
$\widetilde{\boldsymbol{A}} = diag(\underline{\tilde{a}})$.

Note that $\underline{\gamma}$ denotes the nominal values for the gain of the array. Assume that the first sensor of the array is taken as reference and its characteristics are known. It implies that the element $U(1,1)$ of the matrix U will be equal to the gain of the reference sensor, say γ_1, which is known. Therefore the matrix U can be expressed as follows:

$$U = diag(\begin{bmatrix}\gamma_1 \\ \underline{u}\end{bmatrix}) \Rightarrow diag(U) = \begin{bmatrix}\gamma_1 \\ \underline{u}\end{bmatrix} \tag{5}$$

where $\underline{u}$ is the corresponding vector to the rest $N-1$ elements of the matrix U. By using Eqn (4), Eqn (5) can be rewritten as:

$$O^H \cdot \widehat{R_{xx}} \cdot O = \begin{bmatrix}\gamma_1^2 + \sigma^2 & \gamma_1 \cdot \underline{u}^H \\ \gamma_1 \cdot \underline{u} & \underline{u} \cdot \underline{u}^H + \sigma^2\end{bmatrix} \tag{6}$$

From Eqn (5) and (6), the matrix U and the noise power σ^2 can be calculated.

If there are two different pilot sources, then two matrices U_1 and U_2 can be expressed as follows:

$$U_1 = \boldsymbol{\Gamma_1} \cdot \widetilde{\boldsymbol{\Psi}} \cdot \widetilde{A_1} \tag{7a}$$

with $\boldsymbol{\Gamma_1} = diag(\underline{\gamma_1} + \underline{\tilde{\gamma}})$, $\widetilde{\boldsymbol{A_1}} = diag(e^{-j\tilde{r}^T \underline{\boldsymbol{k_1}}})$ and

$$U_2 = \boldsymbol{\Gamma_2} \cdot \widetilde{\boldsymbol{\Psi}} \cdot \widetilde{A_2} \tag{7b}$$

with $\boldsymbol{\Gamma_{21}} = diag(\underline{\gamma_2} + \underline{\tilde{\gamma}})$, $\widetilde{\boldsymbol{A_2}} = diag(e^{-j\tilde{r}^T \underline{\boldsymbol{k_2}}})$

Since the electrical uncertainties are independent of the direction of pilot sources, matrix $\widetilde{\boldsymbol{\Psi}}$ is common for both matrices U_1 and U_2. The following equation can be obtained by using Eqn (7a) and (7b):

$$\angle(U_2^{-1} \cdot U_1) = -diag(\widetilde{r^T} \cdot (\underline{k_1} - \underline{k_2})) \tag{8}$$

Note that $\angle(\cdot)$ denotes the angle of the argument. Eqn (8) can be reexpressed as:

$$\tilde{r}^T \cdot (\underline{k_1} - \underline{k_2}) = diag(\angle(U_2^{-1} \cdot U_1)) \tag{9}$$

For simplicity, $\underline{k_1} - \underline{k_2}$ can be expressed as $\underline{k_1} - \underline{k_2} = [K_{11}\, K_{21}\, K_{31}]^T$. By using the location error in x, y and z coordinates, Eqn (9) becomes:

$$K_{11}\underline{\tilde{x}} + K_{21}\underline{\tilde{y}} + K_{31}\underline{\tilde{z}} = diag(\angle(U_2^{-1} \cdot U_1)) \tag{10}$$

With the assumption that the array is planar (i.e, $\underline{z} = \underline{\tilde{z}} = \underline{0}$), Eqn (10) can be simplified to:

$$K_{11}\underline{\tilde{x}} + K_{21}\underline{\tilde{y}} = diag(\angle(U_2^{-1} \cdot U_1)) \tag{11}$$

A set of N equations with 2N unknowns $(\underline{\tilde{x}}, \underline{\tilde{y}})$ exists in Eqn (11). For a unique solution, therefore, another set of N equations is needed. By using another pilot source, matrix U_3 can be generated as follows:

$$\underline{k_1} - \underline{k_3} = [K_{12}\, K_{22}\, K_{32}]^T$$
$$K_{12}\underline{\tilde{x}} + K_{22}\underline{\tilde{y}} = diag(\angle(U_3^{-1} \cdot U_1)) \tag{12}$$

A new set of N equations is defined in Eqn (12). Therefore, a unique solution for $(\underline{\tilde{x}}, \underline{\tilde{y}})$ can be calculated by using Eqn (11) and (12):

$$\underline{\tilde{y}} = -\frac{K_{11}}{K_{11}K_{22} - K_{12}K_{21}} diag(\angle(U_3^{-1} \cdot U_1)) + \frac{K_{12}}{K_{11}K_{22} - K_{12}K_{21}} diag(\angle(U_2^{-1} \cdot U_1)) \tag{13a}$$

$$\underline{\tilde{x}} = -\frac{1}{K_{11}} \cdot diag(\angle(U_2^{-1} \cdot U_1)) - \frac{K_{21}}{K_{11}} \cdot \underline{\tilde{y}} \tag{13b}$$

Note that at least two out of three pilot sources are placed at different azimuth angles so that Eqn (11) and (12) are independent. Now the geometrical errors are estimated. Next, it is needed to estimate electrical errors, which are the gain and phase of array elements. Note that one of the three matrices U_1, U_2 and U_3 can be used to estimated the electrical errors. Consider that matrices with $\widetilde{\boldsymbol{\Psi}}$ and $\widetilde{\boldsymbol{A_1}}$ are complex matrices with unit power. From this factor, the real matrix Γ_1 can be estimated. It implies that:

$$\begin{aligned}\Gamma_1 = abs(\mathrm{U}_1) &\Rightarrow \underline{\gamma_1} + \tilde{\underline{\gamma}} = \mathrm{diag}(abs(\mathrm{U}_1)) \\ &\Rightarrow \tilde{\underline{\gamma}} = diag(abs(\mathrm{U}_1)) - \underline{\gamma_1}\end{aligned} \tag{14}$$

Thus, the estimated gain error, $\tilde{\underline{\gamma}}$, is calculated by using Eqn (14). To estimate phase errors, then, it is needed to calculate the matrix $\widetilde{\mathbf{A}_1}$ based on the estimated location errors:

$$\begin{aligned}\tilde{\Psi} &= \Gamma_1^{-1} \cdot U_1 \cdot \widetilde{A_1^{-1}} \\ &\Rightarrow e^{j\tilde{\underline{\phi}}} = diag(\Gamma_1^{-1} \cdot U_1 \cdot \widetilde{A_1^{-1}}) \\ &\Rightarrow \tilde{\underline{\phi}} = -j \cdot \ln(diag(\Gamma_1^{-1} \cdot U_1 \cdot \widetilde{A_1^{-1}}))\end{aligned} \tag{15}$$

2-2. Ng and Lie' s method

Consider an un-calibrated array system of L sensors which operates in the presence of M pilot sources at azimuth angle of θ_j and elevation angle of ϕ_j for $j=1,2,\cdots,M$. The spatial spectrum of the MUSIC estimator is defined as:

$$P_{MUSIC}(\theta) = (a(\theta,\phi,g,r)^H E_n E_n^H a(\theta,\phi,g,r))^{-1} \tag{16}$$

where, $a(\theta,\phi,g,r)$ is the steering vector of a pilot source, g is the gain/phase vector, r is the array geometry vector and E_n is a noise eigen-vectors obtained through eigen-decomposition of the data covariance matrix. It is obvious that projection of the signal position vector onto the noise subspace should be equal to zero under the asymptotic condition. This means that, from Eqn (16), for a particular signal source direction θ_j, a set of linear equations can be obtained as:

$$E_n^H a(\theta_j,\phi_j,g,r) = 0 \ \text{ for } \ j=1,2,\cdots,M \tag{17}$$

Using the first-order Taylor series expansion, the true steering vector in any look direction for an un-calibrated array can be approximated as follows:

$$\begin{aligned}a(\theta_j,\phi_j,g,r) = {}& a_0(\theta_j,\phi_j,g,r_0) \\ &+ diag(a_0(\theta_j,\phi_j,g,r_0)) \cdot \triangle_j\end{aligned} \tag{18}$$

where $a_0(\theta_j,\phi_j,g,r_0)$ is the nominal steering vector and $diag(a_0(\theta_j,\phi_j,g,r_0)) \cdot \triangle_j$ is the error term, where $\triangle_j$ is the complex vector defined as:

$$\triangle_j = \triangle_j(\theta_j,\phi_j,g,\tilde{r}) = diag[g]e^{j\tilde{r}k(\theta_j,\phi_j)} \tag{19a}$$

This can be rewritten as follows:

$$\triangle_j = \triangle_j(\theta_j,\phi_j,g,\tilde{r}) = diag[g]e^{j[\tilde{r}k(\theta_j,\phi_j)+\psi]} \tag{19b}$$

where $\psi = [\psi_1, \psi_2, \cdots, \psi_L]^T$.

Substituting Eqn (18) into Eqn (17) give the following expression:

$$\begin{aligned}E_n^H diag(a_0(\theta_j,\phi_j,g,r_0)) \cdot \triangle_j \\ = -E_n^H a_0(\theta_j,\phi_j,g,r_0)\end{aligned} \tag{20}$$

From Eqn (20), it can be seen that if the number of known sources is N, and if the first element of the array sensor is chosen to be the reference element with its complex gain completely known, the following equations are obtained:

$$Q\triangle_j = -P \tag{21a}$$

where Q is a $(N\times(L-M)+1)\times L$ dimensional matrix, which is given by

$$Q = \begin{pmatrix} E_{n1}^H \\ \vdots \\ E_{ni}^H \\ \vdots \\ E_{nN}^H \\ 1\,0\,0\,0\cdots\,0 \end{pmatrix} diag[a_0(\theta_j,\phi_j,g,r_0)] \tag{21b}$$

and P is a $(N\times(L-M)+1)$ dimensional vector, which is defined as

$$P = \begin{pmatrix} E_{n1}^H \\ \vdots \\ E_{ni}^H \\ \vdots \\ E_{nN}^H \\ 0 \end{pmatrix} a_0(\theta_j,\phi_j,g,r_0) \tag{21c}$$

Therefore the solution vector is calculated by the following equation:

$$\triangle = -Q^+ P \tag{22}$$

where $[\,]^{+}$ denotes pseudo-inverse operation and $\triangle = [\triangle_1, \triangle_2, \cdots, \triangle_{N+1}]$.

Any one of the $\triangle_j$ can be used to estimate the gain error of array sensor:

$$|g| = |\triangle_j| \tag{23}$$

Then array geometry and phase can be estimated by using the following equation:

$$[r \,:\, \psi] = -j\log(\triangle)K_a^{-1} \tag{24}$$

where $K_a = \begin{pmatrix} K \\ \cdots \\ 111\ldots1 \end{pmatrix}$.

Ⅲ. Simulation Results

In order to compare the performance of two calibration methods the same simulation setups are made. In this simulation 8-element array sensor is employed. The followings are assumed for the simulation:

● True location - the first sensor is located at the origin of the Cartesian coordinates, i.e, (0, 0, 0). The other sensors are placed with the distance of a unit of half-wavelength along the x-axis.

● Nominal location - sensors are placed away from the true location with some location errors.

● Three pilot sources are placed at azimuth angles of 30, 40 and 120.

● The number of snapshot received at array sensors is 100.

● The value of SNR is from 10dB to 50dB.

Each performance of two calibration techniques is shown in section 3-1 and 3-2. Note that Table 1-6 are generated representatively when SNR is 30dB in which both calibration methods start having almost zero error. In section 3-3, two calibration methods are compared with respect to the RMSE of gain, phase and location when SNR is from 10dB to 50dB.

3-1. Fistas and Manikas' s method

The Fig. 2 shows the actual, nominal and estimated location of array sensors. It is easy to see that the estimated location is almost the same as the actual location. It implies that this calibration method works properly.

In order to analyze the calibration method concretely, the location errors of un-calibrated and calibrated array system are presented in Table 1. Table 2 and Table 3 show the phase errors and gain errors of calibrated array sensors respectively. In comparison of the errors before and after applying the array calibration method, it is obvious that both geometrical and electrical errors are reduced after applying the array calibration methods. For example,

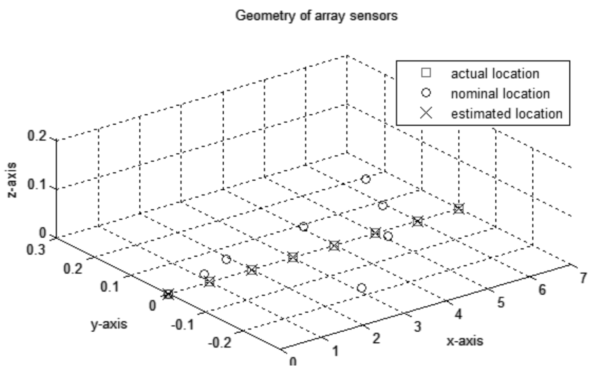

그림 2. 명목상 배열센서 위치 (○), 실제 배열센서 위치 (□), 예측한 배열센서 위치 (X)
Fig. 2. The nominal (○), actual (□) and the estimated (X) array sensor geometry.

표 1. 초기 위치오차와 최종 위치오차 비교
Table 1. Comparison of initial location errors and final location errors.

	Initial location errors		Final location errors ($\times 10^{-3}$)	
	x-axis	y-axis	x-axis	y-axis
element 2	0.1542	-0.0330	0.0162	0.0041
element 3	0.0563	0.0620	0.0333	0.1051
element 4	0.1250	0.1700	0.0720	0.2731
element 5	0.0800	0.0930	0.0755	0.5097
element 6	0.0870	0.0240	0.0429	0.2694
element 7	0.0550	0.0880	0.0022	0.0160
element 8	0.5020	0.1940	0.0029	0.0229
mean	0.1514	0.0949	0.1321	0.1715

표 2. 초기 위상오차와 최종 위상오차 비교
Table 2. Comparison of initial phase errors and final phase errors.

	Initial gain errors	Final gain errors ($\times 10^{-3}$)
element 2	0.0331	0.1478
element 3	0.0375	0.0422
element 4	0.0312	0.0785
element 5	0.0045	0.0632
element 6	0.0441	0.0375
element 7	0.0319	0.0717
element 8	0.0075	0.0551
mean	0.0271	0.0708

표 3. 초기 이득오차와 최종 이득오차 비교
Table 3. Comparison of initial gain errors and final gain errors.

	Initial phase errors	Final phase errors ($\times 10^{-14}$)
element 2	0.0185	0.0250
element 3	0.0074	0.0000
element 4	0.0094	0.0066
element 5	0.0032	0.0000
element 6	0.0026	0.0250
element 7	0.0021	0.3587
element 8	0.0111	0.3587
mean	0.0078	0.1106

the average location errors of un-calibrated array sensors are 0.1514 and 0.0949 in x-axis and y-axis respectively, whereas the average location errors of calibrated array sensors are 0.0001321 and 0.0001715 in x-axis and y-axis respectively. The location errors are significantly reduced by the calibration algorithm.

3-2. Ng and Lie' s method

Table 4, Table 5 and Table 6 show the location errors, phase errors and gain errors of calibrated array sensors respectively. As Fistas and Manikas's method, geometrical and electrical errors are reduced after applying the calibration method designed by Ng and Lie. For example, the average phase errors of un-calibrated array sensors are 0.0271, whereas the average phase errors of calibrated array sensors are 0.00059. The errors are reduced by around 85 %.

표 4. 초기 위치오차와 최종 위치오차 비교
Table 4. Comparison of initial location errors and final location errors.

	Initial location errors		Final location errors ($\times 10^{-3}$)	
	x-axis	y-axis	x-axis	y-axis
element 2	0.1542	0.0330	0.01070	0.01722
element 3	0.0563	0.0620	0.03002	0.01532
element 4	0.1250	0.1700	0.03617	0.00132
element 5	0.0800	0.0930	0.02542	0.01227
element 6	0.0870	0.0240	0.01389	0.00791
element 7	0.0550	0.0880	0.01392	0.00101
element 8	0.5020	0.1940	0.01934	0.00198
mean	0.1513	0.0949	0.02135	0.00814

표 5. 초기 위상오차와 최종 위상오차 비교
Table 5. Comparison of initial phase errors and final phase errors.

	Initial phase errors	Final phase errors ($\times 10^{-1}$)
element 2	0.0331	0.0063
element 3	0.0375	0.0113
element 4	0.0312	0.0020
element 5	0.0045	0.0018
element 6	0.0441	0.0065
element 7	0.0319	0.0103
element 8	0.0075	0.0033
mean	0.0271	0.0059

표 6. 초기 이득오차와 최종 이득오차 비교
Table 6. Comparison of initial gain errors and final gain errors.

	Initial gain errors	Final gain errors ($\times 10^{-3}$)
element 2	0.0185	0.0422
element 3	0.0074	0.1292
element 4	0.0094	0.1819
element 5	0.0032	0.0499
element 6	0.0026	0.0396
element 7	0.0021	0.0197
element 8	0.0111	0.0085
mean	0.0076	0.0673

3-3. Comparison of two calibration methods

For the next simulation, different values of SNR from 10dB to 50dB are applied to two calibration methods. The rest of the simulation parameters are kept. Then, the RMSE of location, gain and phase are calculated and plotted to compare the performance of

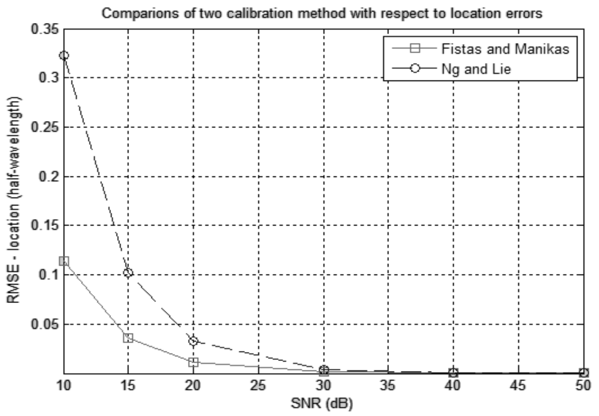

그림 3. 두 가지 보정기술의 위치 평균 제곱근 편차 비교
Fig. 3. Comparison of two calibration with respect to the RMSE of location.

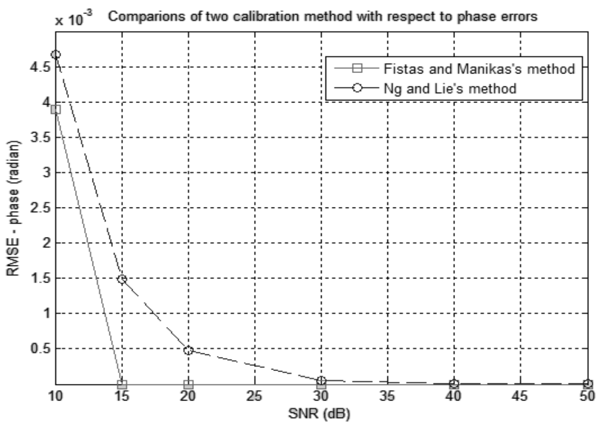

그림 4. 두 가지 보정기술의 위상 평균 제곱근 편차 비교
Fig. 4. Comparison of two calibration with respect to the RMSE of phase.

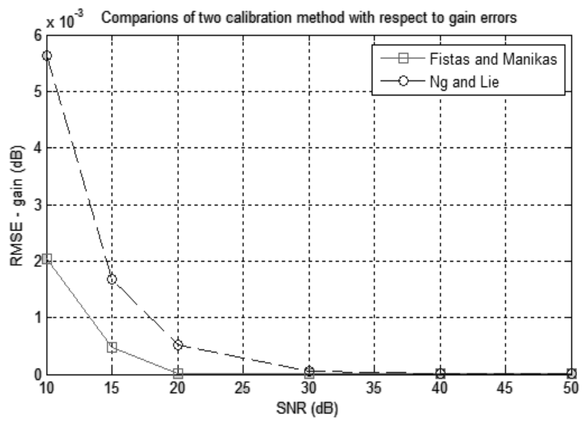

그림 5. 두 가지 보정기술의 이득 평균 제곱근 편차 비교
Fig. 5. Comparison of two calibration with respect to the RMSE of gain.

two calibration techniques. The Fig. 3-5 display the RMSE of location, phase and gain with different values of SNR respectively. It is obvious that the performance of two calibration methods decreases as the value of SNR decreases. Then it can be confirmed that both calibration techniques have almost zero error when SNR is more than 30dB. With comparison of two methods, Fistas and Manikas's method has less error even though the value of SNR is low. It implies that Fistas and Manikas's method is more robust than Ng and Lie's method in the noise environment.

Ⅳ. Conclusion

The geometrical and electrical errors are inherent in manufacturing process of array sensors. Two different array calibration methods in this paper estimate errors and calibrate array sensors with respect to location, gain and phase simultaneously. Through the computer-based simulation, it has been shown that the array calibration technique designed by Fistas and Manikas is more robust against noise than the one designed by Ng and Lie in the noise environment. There are constant numbers in the last row of the matrix Q and P in Ng and Lie′s method. These numbers are fixed on whatever noise is applied. This might be a reason why Ng and Lie′s method is less robust than Fistas and Manikas′s method in the noise environment.

Moreover, both calibration algorithms would be improved by using an adaptive antenna array/an adaptive array processing with the use of feedback to optimize the performance of array system. There are various optimization criteria such as maximizing the SNR at the array output and minimizing the RMSE between the actual array output and the estimated array output. However, it is needed to analyse trade-offs between improved noise robustness of the calibrated array and processing complexity of the calibration algorithm.

References

[1] G. Efstathopoulos, G. Elissaios and A. Manikas, “The effect of uncertainties on the performance of array systems,” IEEE 18th International symposium on Personal, Indoor and Mobile Radio Communication, pp. 1-5, Sept. 2007.

[2] Don H. Johnson and Dan E. Dudgeon, “Array signal processing conception and techniques,” Prentice_Hall, 1993.

[3] J. T. Lo and S. L. Marple Jr., “Eigenstructure methods for array sensor localization,” IEEE proc. ICASSP, Vol. 12, pp. 2260-2263, April 1987.

[4] L. Seymour, C. Cowan and P. Grant, “Bearing estimation in the presence of sensor positioning error,” IEEE proc. ICASSP, Vol. 12, pp. 2264-2267, April 1987.

[5] A. J. Weiss and B. Friedlander, “Array shape calibration using sources in unknown locations- A maximum likelihood approach,” IEEE Trans. on ASSP, Vol. 37, no. 12, pp. 1958-1966, Dec. 1989.

[6] A. J. Weiss and B. Friedlander, “Array shape calibration using eigenstructure methods,” Signals, Systems and Computers, Vol. 2 pp. 925-929, 1989

[7] Ming Zhang and Zhao-Da Zhu, “Array shape calibration using sources in known directions,” Aerospace and Electronics Conference, NEACON 1993, Vol. 1, pp. 70-73, May 1993.

[8] S. H. Lee, C. S. Ryu and K. K. Lee, “Near-field source localization using bottom-mounted linear sensor array in multipath environment,” IEE proc. Radar, Sonar and Navigation, Vol. 149, no. 4, pp. 202-206, August 2002.

[9] J. Fuchs, “Shape Calibration for a Nominally Linear Equi-spaced Array,” IEEE proc. ICASSP, Vol. 4, pp. 300-303, April 1993.

[10] B. P. Ng, M. H. Er and C. Kot, “Array gain/phase calibration techniques for adaptive beamforming and direction finding,” IEE proc. Radar, Sonar and Navigation, Vol. 141, no. 1, Feb. 1994.

[11] B. Friedlander and A. J. Weiss, “Eigenstructure methods for direction finding with sensor and gain uncertainties,” IEEE proc. ICASSP, Vol. 5, pp. 2681-2684, April 1988.

[12] Chen Deli, Zhang Cong, Tao Huamin and Lu Huanzhang, “UCA gain/phase calibration in the presence of multipath based on weighted subspace fitting,” Information and Automation, 2008. ICIA 2008. International Conference on, pp. 1364-1367, June 2008.

[13] B. Friedlander and A. J. Weiss, “Self-calibration for high resolution array processing,” in Advances in Spectrum and Array Processing (S. Haykins, Ed.). Englewood Cliffs, NJ: Prentice Hill, 1991, ch. 10, Vol. II.

[14] Boon Poh Ng, Joni Polili Lie, Meng Hwa Er and Aigang Feng, “A practical simple geometry and gain/phase calibration technique for antenna array processing,” IEEE Trans. on Antennas and Propagation, Vol. 57, No. 7, pp. 1963-1972, July 2009.

[15] N. Fistas and A. Manikas, “ A new general global calibration method,” IEEE proc. ICASSP, Vol. 4, no. 1, pp. 73-76, April 1994.

[16] Chang Soo Ryu, "3-Dimensional Linear Sensor Array Calibration Using Known Sources", Journal of IEEK- TE, Vol. 41, no. 3, pp. 47-52, Sep. 2004.

저 자 소 개

유 성 기(정회원)
2010년 University of Surrey, 통신학과 학사 졸업.
2012년 Imperial College London, 통신 신호처리학과 석사 졸업
2012년~현재 한국전기연구원 연구원
<주관심분야 : 배열신호처리, 생체신호처리, 배열안테나>

신 기 영(정회원)-교신저자
2004년 성균관대학교 바이오메카트로닉스학과 학사 졸업.
2006년 성균관대학교 생명공학과 석사 졸업.
2011년 성균관대학교 생명공학과 박사 졸업.
2011년~현재 한국전기연구원 선임연구원
<주관심분야 : 신호처리, 의료영상처리, 컴퓨터비전>

이 태 범(정회원)
1998년 을지대학교 임상병리학과 학사 졸업.
2004년 서울대학교 공중보건학과 석사 졸업.
2010년 서울가톨릭대학교 공중보건학과 박사 졸업.
2010년~현재 한국전기연구원 선임연구원
<주관심분야 : 임상병리, 산업보건, 생체신호계측>